Received: 17 September 2019 | Revised: 13 December 2019 | Accepted: 8 January 2020

DOI: 10.4218/etrij.2019-0431

ORIGINAL ARTICLE

ETRI Journal WILEY

On the performance of improved quadrature spatial modulation

Tasnim Holoubi[1] | **Sheriff Murtala**[1] | **Nishal Muchena**[1] | **Manar Mohaisen**[2]

[1]Department of EEC Engineering, KOREATECH, Cheonan, Rep. of Korea

[2]Department of Computer Science, Northeastern Illinois University, Chicago, IL, USA

Correspondence
Manar Mohaisen, Department of Computer Science, Northeastern Illinois University, Chicago, IL, USA.
Email: m-mohaisen@neiu.edu

Quadrature spatial modulation (QSM) utilizes the in-phase and quadrature spatial dimensions to transmit the real and imaginary parts of a single signal symbol, respectively. The improved QSM (IQSM) transmits two signal symbols per channel use through a combination of two antennas for each of the real and imaginary parts. The main contributions of this study can be summarized as follows. First, we derive an upper bound for the error performance of the IQSM. We then design constellation sets that minimize the error performance of the IQSM for several system configurations. Second, we propose a double QSM (DQSM) that transmits the real and imaginary parts of two signal symbols through any available transmit antennas. Finally, we propose a parallel IQSM (PIQSM) that splits the antenna set into equal subsets and performs IQSM within each subset using the same two signal symbols. Simulation results demonstrate that the proposed constellations significantly outperform conventional constellations. Additionally, DQSM and PIQSM provide a performance similar to that of IQSM while requiring a smaller number of transmit antennas and outperform IQSM with the same number of transmit antennas.

KEYWORDS

constellation design, MIMO system, multivariate optimization, pairwise error probability, quadrature spatial modulation

1 | INTRODUCTION

Index modulation (IM) refers to a group of multiple-input multiple-output (MIMO) techniques that convey information through the indices of available communication system resources [1,2]. Spatial modulation (SM) is an IM technique that uses the indices of transmit and/or receive antennas to convey additional information [3]. In conventional SM, a single antenna, whose index is a spatial symbol, is activated to transmit a signal symbol drawn from a conventional constellation (eg, quadrature amplitude modulation (QAM) or phase shift keying (PSK)). Therefore, SM only requires one radio-frequency (RF) chain to provide satisfactory MIMO capacity. Several works that extend conventional SM were introduced in [4–8].

In conventional SM, the number of transmit antennas must be a power of two. To overcome this limitation, generalized SM (GSM) was proposed in [9], where a combination of antennas was activated to transmit a single signal symbol at each channel use. To further increase spectral efficiency, multiple-active SM (MA-SM) uses a combination of transmit antennas to transmit independent signal symbols at each channel use [10]. The resulting performance improvement comes at the cost of an increased number of RF chains and increased receiver complexity.

Quadrature SM (QSM) uses the in-phase spatial dimension to transmit the real part of a signal symbol and the quadrature dimension to transmit the imaginary part [11]. Therefore, QSM effectively doubles spatial spectral efficiency while requiring only a single RF chain. Detection algorithms and constellation design for QSM were addressed in [12] and [13], respectively. The spectral efficiency of QSM can be further enhanced by transmitting multiple signal

symbols at each channel use (eg, precoding-aided QSM [14] and extended QSM [15]).

In complex QSM (CQSM), two signal symbols drawn from two disjoint modulation sets are transmitted at each channel use [16]. The first modulation set can be any conventional QAM/PSK constellation and the second is an optimally rotated version of the first. CQSM was improved in [17] and modulation set optimization for improved CQSM was addressed in [18]. Furthermore, two generalized algorithms for CQSM were proposed in [19].

To increase the spectral efficiency of QSM, an improved QSM (IQSM) method that transmits two signal symbols at each time instance was proposed in [20]. In IQSM, the real and imaginary parts are transmitted using a combination of two antennas and both signal symbols are drawn from the same modulation set.

Recently, a parallel implementation of SM using antenna grouping was introduced in [21–24]. The available antenna set was divided into equal subsets and conventional SM was performed in each of the subsets using either the same signal symbol or different symbols. The constellation design for parallel SM was addressed in [25]. Similarly, a parallel implementation of QSM, referred to as generalized QSM (GQSM), was proposed in [26], where independent signal symbols were transmitted through each antenna subset. The spectral efficiency of GQSM linearly increases with the number of subsets, but the required number of RF chains also increases. To maintain a simple transmitter design with one RF chain, parallel QSM was proposed in [27,28], where the same signal symbol was used to perform QSM in all antenna subsets.

The main contributions of our study can be summarized as follows:

- We derive an upper bound for the pairwise error probability (PEP) of IQSM. Based on the obtained upper bound, we formulate constellation design as a multi-objective optimization problem. The proposed constellation design reduces asymptotic error performance.
- We propose double QSM (DQSM), where the real and imaginary parts of two signal symbols are transmitted from designated antennas, whose indices carry additional information. The two signal symbols are drawn from two different modulation sets such that the first set is any conventional QAM/PSK and the second set is a rotated version of the first. The optimal rotation angle that minimizes the error rate is identified through extensive Monte Carlo simulations. Initial results for DQSM were analyzed in [29].
- Finally, we propose a parallel IQSM (PIQSM) system that splits the antenna set into equal subsets and performs IQSM independently in each subset using the same signal symbols. Therefore, PIQSM inherits the main characteristics of IQSM while requiring a much smaller number of antennas to achieve a given spectral efficiency.

Simulation results demonstrate that the proposed constellation for IQSM outperforms QAM and PSK schemes by up to 2.5 dB and 8 dB, respectively. Both DQSM and PIQSM require a smaller number of transmit antennas to achieve a given spectral efficiency and improve spectral efficiency for an equal number of transmit antennas. It should be noted that IQSM, DQSM, and PIQSM each require two RF chains. Assuming QPSK modulation, DQSM requires 14 fewer transmit antennas than IQSM to achieve a spectral efficiency of 24 bits per channel use (bpcu). Additionally, PIQSM reduces the required number of transmit antennas to achieve a spectral efficiency of 22 bpcu by 18. For the same number of transmit antennas, DQSM and PIQSM outperform IQSM by approximately 2 dB and 3 dB, respectively.

The remainder of this paper is organized as follows. In Section 2, we describe the proposed system model and review-related works. Theoretical performance analysis and the constellation design of IQSM are addressed in Sections 3 and 4, respectively. We introduce DQSM in Section 5 and PIQSM in Section 6. The receiver complexity of the proposed schemes is analyzed in Section 7. Simulation results are presented and analyzed in Section 8. Conclusions are drawn in Section 9.

2 | SYSTEM MODEL AND RELATED WORKS

Consider a MIMO system in which a base station with N_t transmit antennas communicates with a single mobile station with n_R receive antennas. The $n_R \times N_t$ channel matrix $\mathbf{H}$ and $n_R \times 1$ noise vector $\mathbf{n}$ have i.i.d. elements of circularly symmetric complex Gaussian variables with zero mean and variances of one and σ^2, respectively. The $N_t \times 1$ transmitted vector $\mathbf{s}$ has a unit norm such that the signal-to-noise ratio (SNR) is $1/\sigma^2$. The signal symbols are drawn from modulation sets of size L, where $L = 2^q$ and q is the number of bits per signal symbol.

2.1 | Quadrature spatial modulation

In QSM, the real and imaginary parts of a signal symbol s_k are transmitted over the in-phase and quadrature dimensions, respectively. At each channel use, the incoming information bits are divided into three subsets. The first set is used to select s_k and the remaining subsets modulate the antenna indices $l_{\Re}$ and $l_{\Im}$, which are used to transmit the real and imaginary parts $s_{k_{\Re}}$ and $s_{k_{\Im}}$, respectively. Therefore, the received vector is defined as follows:

$$\mathbf{y}=\mathbf{h}_{l_{\Re}}s_{k_{\Re}}+j\mathbf{h}_{l_{\Im}}s_{k_{\Im}}+\mathbf{n}, \tag{1}$$

where $\mathbf{h}_l$ is the l-th column of the channel matrix $\mathbf{H}$. Accordingly, QSM achieves a total spectral efficiency of $\left(2N_{\text{QSM}}+q\right)$ bpcu, where $N_{\text{QSM}}=\log_2\left(N_{\text{t}}\right)$ is the number of bits per spatial symbol.

2.2 | Multi-active spatial modulation

In MA-SM, an antenna combination of length n_{U} selected from N_{t} available antennas is used to transmit n_{U} independent signal symbols at each channel use. Among the available $\binom{N_{\text{t}}}{n_{\text{U}}}$ combinations, $2^{N_{\text{MA-SM}}}$ combinations can be used for transmission, where $N_{\text{MA-SM}}=\left\lfloor\log_2\binom{N_{\text{t}}}{n_{\text{U}}}\right\rfloor$. The $\binom{\cdot}{\cdot}$ and $\lfloor\cdot\rfloor$ operators denote the binomial coefficient and floor function, respectively. The received vector is defined as follows:

$$\mathbf{y}=\sum_{i=1}^{n_t}\mathbf{h}_{l_i}s_i+\mathbf{n}, \tag{2}$$

where $\boldsymbol{l}_j=\{l_1,...,l_{n_U}\}$ is the j-th combination among the valid combinations. MA-SM achieves a total spectral efficiency of $\left(N_{\text{MA-SM}}+n_{\text{U}}\times q\right)$ bpcu.

2.3 | Improved quadrature spatial modulation

IQSM transmits the real and imaginary parts of two signal symbols s_{k_1} and s_{k_2} through pairs of antennas. There are $2^{N_{\text{IQSM}}}$ valid combinations that can be used for the transmission of the real or imaginary parts, where $N_{\text{IQSM}}=\left\lfloor\log_2\binom{N_{\text{t}}}{2}\right\rfloor$. At each channel use, $s_{k_{1\Re}}$ and $s_{k_{2\Re}}$ are transmitted through the in-phase antenna combination $\boldsymbol{l}_{\Re}=\left\{l_{1\Re},l_{2\Re}\right\}$. Similarly, $s_{k_{1\Im}}$ and $s_{k_{2\Im}}$ are transmitted through the quadrature antenna combination $\boldsymbol{l}_{\Im}=\left\{l_{1\Im},l_{2\Im}\right\}$. Assuming that $l_{1\Re}<l_{2\Re}$ and $l_{1\Im}<l_{2\Im}$, the received vector is defined as follows:

$$\mathbf{y}=\mathbf{h}_{l_{1\Re}}s_{k_{1\Re}}+\mathbf{h}_{l_{2\Re}}s_{k_{2\Re}}+j\mathbf{h}_{l_{1\Im}}s_{k_{1\Im}}+j\mathbf{h}_{l_{2\Im}}s_{k_{2\Im}}+\mathbf{n}. \tag{3}$$

Accordingly, the spectral efficiency of IQSM is $2\left(N_{\text{IQSM}}+q\right)$ bpcu.

3 | PERFORMANCE ANALYSIS

Let $\mathbf{g}=\mathbf{Hs}$ and $\hat{\mathbf{g}}=\mathbf{H}\hat{\mathbf{s}}$ be two noiseless received codewords corresponding to the transmitted vectors $\mathbf{s}$ and $\hat{\mathbf{s}}$, respectively, for any MIMO system. The conditional PEP is defined as a function of the Gaussian tail function $Q(.)$ as follows [30]:

$$\Pr\left[\mathbf{g}\to\hat{\mathbf{g}}|\mathbf{H}\right]=Q\left(\sqrt{\frac{\|\mathbf{g}-\hat{\mathbf{g}}\|^2}{2\sigma_n^2}}\right), \tag{4}$$

where $d_{\text{rx}}^2=\|\mathbf{g}-\hat{\mathbf{g}}\|^2$ is the squared Euclidean distance (ED) at the receiver. Applying the expectation of (4) over the channel $\mathbf{H}$ yields the unconditional PEP (UPEP), which is defined as follows:

$$\Pr\left[\mathbf{g}\to\hat{\mathbf{g}}\right]=\mu^{n_{\text{R}}}\sum_{l=0}^{n_{\text{R}}-1}\binom{n_{\text{R}}-1+l}{l}[1-\mu]^l, \tag{5}$$

where

$$\mu=\frac{1}{2}\left(1-\sqrt{\frac{\gamma\cdot d_{\text{tx}}^2}{4+\gamma\cdot d_{\text{tx}}^2}}\right), \tag{6}$$

and $d_{\text{tx}}^2=\|\mathbf{s}-\hat{\mathbf{s}}\|^2$ and γ are the squared ED at the transmitter and the SNR, respectively. Note that

$$\mathbb{E}_{\mathbf{H}}\left\{d_{\text{rx}}^2\right\}=(\mathbf{s}-\hat{\mathbf{s}})^H\mathbf{H}^H\mathbf{H}(\mathbf{s}-\hat{\mathbf{s}})=d_{\text{tx}}^2, \tag{7}$$

where $\mathbb{E}\{\cdot\}$ and $(\cdot)^H$ denote the expected value and Hermitian transpose, respectively.

By calculating the average of all pairwise probabilities, the union bound of UPEP can be defined as follows:

$$\Pr[e]\leqslant\frac{1}{2^M}\sum_{j=1}^{2^M}\sum_{k=1}^{2^M}\Pr\left[\mathbf{g}_j\to\hat{\mathbf{g}}_k\right]. \tag{8}$$

Accordingly, the average bit error rate (BER) is defined as follows:

$$\text{Pr}_e\leqslant\frac{1}{M2^M}\sum_{j=1}^{2^M}\sum_{k=1}^{2^M}\text{D}_{\mathbf{s},\hat{\mathbf{s}}}\Pr\left[\mathbf{g}_j\to\hat{\mathbf{g}}_k\right], \tag{9}$$

where $\text{D}_{\mathbf{s},\hat{\mathbf{s}}}$ is the Hamming distance, which is defined as the number of errors associated with the event $\left[\mathbf{g}_j\to\hat{\mathbf{g}}_k\right]$, and M is the total spectral efficiency of the system.

In the next section, we derive an upper bound for the pairwise error performance of IQSM. The derived upper bound is formulated as a sum of several objective functions that can be solved to obtain the proposed constellation.

4 | CONSTELLATION DESIGN FOR IQSM

At high SNRs, the asymptotic UPEP can generally be approximated as follows [31]:

$$\Pr\left[\mathbf{g}\to\hat{\mathbf{g}}\right]\approx\frac{2^{2n_{\mathrm{R}}-1}\Gamma\left(n_{\mathrm{R}}+0.5\right)}{\sqrt{\pi}n_{\mathrm{R}}!}\left(\frac{1}{\gamma d_{\mathrm{tx}}^2}\right)^{n_{\mathrm{R}}}=\binom{2n_{\mathrm{R}}-1}{n_{\mathrm{R}}}\gamma^{-n_{\mathrm{R}}}\left(d_{\mathrm{tx}}^2\right)^{-n_{\mathrm{R}}}. \tag{10}$$

By substituting (10) into (8), the average union bound on the pairwise error probability can be defined as follows:

$$\begin{aligned}\Pr[e]&\leqslant\frac{1}{2^M}\sum_{j=1}^{2^M}\sum_{k=1}^{2^M}\Pr\left[\mathbf{g}_j\to\hat{\mathbf{g}}_k\right]\\&=\binom{2n_{\mathrm{R}}-1}{n_{\mathrm{R}}}\frac{\gamma^{-n_{\mathrm{R}}}}{2^M}\sum_{j=1}^{2^M}\sum_{k=1}^{2^M}\left(d_{j,k(\mathrm{tx})}^2\right)^{-n_{\mathrm{R}}}\\&=\binom{2n_{\mathrm{R}}-1}{n_{\mathrm{R}}}\frac{\gamma^{-n_{\mathrm{R}}}}{L^2}\sum_{i=1}^{B}f_i\Omega_i,\end{aligned} \tag{11}$$

where B is the number of unique expressions of d_{tx}^2 and f_i is the frequency corresponding to the i-th expression Ω_i.

Based on (11), the error performance of the IQSM system is a function of d_{tx}^2 and n_{R}. While (11) does not explicitly depend on N_{t}, both f_i and Ω_i do, as will be shown in the following section. For fixed values of n_{R} and N_{t}, d_{tx}^2 is the only variable that affects the error performance in (11). Because the real and imaginary parts are transmitted via orthogonal carriers, inter-carrier interference is mitigated. Therefore, the analyses of the contributions of the real and imaginary parts to the Ω functions are independent and identical.

Let the indices of the antennas used to transmit the real parts be $l_{1\Re}$ and $l_{2\Re}$, and let the estimated antenna indices be $\hat{l}_{1\Re}$ and $\hat{l}_{2\Re}$. It is worth noting that because $l_{1\Re}$ and $l_{2\Re}$ belong to the same combination, $l_{1\Re}\neq l_{2\Re}$ and $\hat{l}_{1\Re}\neq\hat{l}_{2\Re}$. According to (3), the number of variables associated with the real parts is four ($l_{1\Re}$, $l_{2\Re}$, $\hat{l}_{1\Re}$, and $\hat{l}_{2\Re}$). Therefore, there are six relational conditions between these four variables. These relationships are defined as follows:

$$\begin{aligned}&l_{1\Re}\overset{?}{=}l_{2\Re},\ l_{1\Re}\overset{?}{=}\hat{l}_{1\Re},\ l_{1\Re}\overset{?}{=}\hat{l}_{2\Re},\\&l_{2\Re}\overset{?}{=}\hat{l}_{1\Re},\ l_{2\Re}\overset{?}{=}\hat{l}_{2\Re},\ \hat{l}_{1\Re}\overset{?}{=}\hat{l}_{2\Re}.\end{aligned} \tag{12}$$

For $l_{1\Re}\neq l_{2\Re}$ and $\hat{l}_{1\Re}\neq\hat{l}_{2\Re}$, (12) can be simplified to four relational conditions as follows:

$$l_{1\Re}\overset{?}{=}\hat{l}_{1\Re},\ l_{1\Re}\overset{?}{=}\hat{l}_{2\Re},\ l_{2\Re}\overset{?}{=}\hat{l}_{1\Re},\ l_{2\Re}\overset{?}{=}\hat{l}_{2\Re}. \tag{13}$$

Intuitively, there is a total of 16 relational statements. However, only six of them are valid and used to compute $\Lambda_{\Re j}=\left\|\mathbf{s}_{\Re}-\hat{\mathbf{s}}_{\Re}\right\|^2$; $j=1,...,6$. The terms $\Lambda_{\Re}$ and $\Lambda_{\Im}$, which will be derived later, are used to compute the Ω terms. The six valid $\Lambda_{\Re j}$ are defined as follows:

$$\begin{aligned}\Lambda_{\Re 1}&=|s_{k_{1\Re}}|^2+|s_{\hat{k}_{1\Re}}|^2+|s_{k_{2\Re}}|^2+|s_{\hat{k}_{2\Re}}|^2\\&\quad\text{if}\quad(l_{1\Re}\neq\hat{l}_{1\Re},l_{1\Re}\neq\hat{l}_{2\Re},l_{2\Re}\neq\hat{l}_{1\Re},l_{2\Re}\neq\hat{l}_{2\Re})\\\Lambda_{\Re 2}&=|s_{k_{1\Re}}-s_{\hat{k}_{1\Re}}|^2+|s_{k_{2\Re}}|^2+|s_{\hat{k}_{2\Re}}|^2\\&\quad\text{if}\quad(l_{1\Re}=\hat{l}_{1\Re},l_{1\Re}\neq\hat{l}_{2\Re},l_{2\Re}\neq\hat{l}_{1\Re},l_{2\Re}\neq\hat{l}_{2\Re})\\\Lambda_{\Re 3}&=|s_{k_{1\Re}}|^2+|s_{\hat{k}_{1\Re}}|^2+|s_{k_{2\Re}}-s_{\hat{k}_{2\Re}}|^2\\&\quad\text{if}\quad(l_{1\Re}\neq\hat{l}_{1\Re},l_{1\Re}\neq\hat{l}_{2\Re},l_{2\Re}\neq\hat{l}_{1\Re},l_{2\Re}=\hat{l}_{2\Re})\\\Lambda_{\Re 4}&=|s_{k_{1\Re}}-s_{\hat{k}_{2\Re}}|^2+|s_{k_{2\Re}}|^2+|s_{\hat{k}_{1\Re}}|^2\\&\quad\text{if}\quad(l_{1\Re}\neq\hat{l}_{1\Re},l_{1\Re}=\hat{l}_{2\Re},l_{2\Re}\neq\hat{l}_{1\Re},l_{2\Re}\neq\hat{l}_{2\Re})\\\Lambda_{\Re 5}&=|s_{k_{1\Re}}|^2+|s_{\hat{k}_{2\Re}}|^2+|s_{k_{2\Re}}-s_{\hat{k}_{1\Re}}|^2\\&\quad\text{if}\quad(l_{1\Re}\neq\hat{l}_{1\Re},l_{1\Re}\neq\hat{l}_{2\Re},l_{2\Re}=\hat{l}_{1\Re},l_{2\Re}\neq\hat{l}_{2\Re})\\\Lambda_{\Re 6}&=|s_{k_{1\Re}}-s_{\hat{k}_{1\Re}}|^2+|s_{k_{2\Re}}-s_{\hat{k}_{2\Re}}|^2\\&\quad\text{if}\quad(l_{1\Re}=\hat{l}_{1\Re},l_{1\Re}\neq\hat{l}_{2\Re},l_{2\Re}\neq\hat{l}_{1\Re},l_{2\Re}=\hat{l}_{2\Re}).\end{aligned} \tag{14}$$

To simplify the following derivation, we define $\mathbf{\Lambda}_{\Re}=\left\{\Lambda_{\Re 1},...,\Lambda_{\Re 6}\right\}$. Similarly, the terms $\mathbf{\Lambda}_{\Im j}=\left\|\mathbf{s}_{\Im}-\hat{\mathbf{s}}_{\Im}\right\|^2$ are defined as follows:

$$\begin{aligned}\Lambda_{\Im 1}&=|s_{k_{1\Im}}|^2+|s_{\hat{k}_{1\Im}}|^2+|s_{k_{2\Im}}|^2+|s_{\hat{k}_{2\Im}}|^2\\&\quad\text{if}\quad(l_{1\Im}\neq\hat{l}_{1\Im},l_{1\Im}\neq\hat{l}_{2\Im},l_{2\Im}\neq\hat{l}_{1\Im},l_{2\Im}\neq\hat{l}_{2\Im})\\\Lambda_{\Im 2}&=|s_{k_{1\Im}}-s_{\hat{k}_{1\Im}}|^2+|s_{k_{2\Im}}|^2+|s_{\hat{k}_{2\Im}}|^2\\&\quad\text{if}\quad(l_{1\Im}=\hat{l}_{1\Im},l_{1\Im}\neq\hat{l}_{2\Im},l_{2\Im}\neq\hat{l}_{1\Im},l_{2\Im}\neq\hat{l}_{2\Im})\\\Lambda_{\Im 3}&=|s_{k_{1\Im}}|^2+|s_{\hat{k}_{1\Im}}|^2+|s_{k_{2\Im}}-s_{\hat{k}_{2\Im}}|^2\\&\quad\text{if}\quad(l_{1\Im}\neq\hat{l}_{1\Im},l_{1\Im}\neq\hat{l}_{2\Im},l_{2\Im}\neq\hat{l}_{1\Im},l_{2\Im}=\hat{l}_{2\Im})\\\Lambda_{\Im 4}&=|s_{k_{1\Im}}-s_{\hat{k}_{2\Im}}|^2+|s_{k_{2\Im}}|^2+|s_{\hat{k}_{1\Im}}|^2\\&\quad\text{if}\quad(l_{1\Im}\neq\hat{l}_{1\Im},l_{1\Im}=\hat{l}_{2\Im},l_{2\Im}\neq\hat{l}_{1\Im},l_{2\Im}\neq\hat{l}_{2\Im})\\\Lambda_{\Im 5}&=|s_{k_{1\Im}}|^2+|s_{\hat{k}_{2\Im}}|^2+|s_{k_{2\Im}}-s_{\hat{k}_{1\Im}}|^2\\&\quad\text{if}\quad(l_{1\Im}\neq\hat{l}_{1\Im},l_{1\Im}\neq\hat{l}_{2\Im},l_{2\Im}=\hat{l}_{1\Im},l_{2\Im}\neq\hat{l}_{2\Im})\\\Lambda_{\Im 6}&=|s_{k_{1\Im}}-s_{\hat{k}_{1\Im}}|^2+|s_{k_{2\Im}}-s_{\hat{k}_{2\Im}}|^2\\&\quad\text{if}\quad(l_{1\Im}=\hat{l}_{1\Im},l_{1\Im}\neq\hat{l}_{2\Im},l_{2\Im}\neq\hat{l}_{1\Im},l_{2\Im}=\hat{l}_{2\Im}).\end{aligned} \tag{15}$$

In set form, we define $\mathbf{\Lambda}_{\Im}=\left\{\Lambda_{\Im 1},...,\Lambda_{\Im 6}\right\}$ for use in the following analysis.

We assume that the valid combinations used for transmission are selected at random. The corresponding frequency for each term in $\mathbf{\Lambda}_{\Re}$ or $\mathbf{\Lambda}_{\Im}$ for the entire set of combinations of size $\binom{N_{\mathrm{t}}}{2}$ is defined as follows:

$$\begin{aligned}f_1&=\tfrac{1}{2}\left(N_{\mathrm{t}}-2\right)\left(N_{\mathrm{t}}-3\right)&\quad f_2&=f_3=\tfrac{2}{3}\left(N_{\mathrm{t}}-2\right)\\f_4&=f_5=\tfrac{1}{3}\left(N_{\mathrm{t}}-2\right)&\quad f_6&=1.\end{aligned} \tag{16}$$

The Ω expressions are obtained from the Minkowski sum of $\mathbf{\Lambda}_{\Re}$ and $\mathbf{\Lambda}_{\Im}$, and formulated as follows:

$$\Omega_i=\sum_{k_1,\hat{k}_1}^{L}\sum_{k_2,\hat{k}_2}^{L}\left[\Lambda_i\right]^{-n_{\mathrm{R}}}, \tag{17}$$

where $\mathbf{\Lambda} = \{\Lambda_1, ..., \Lambda_B\}$ is the resulting set from the Minkowski sum and $B = |\mathbf{\Lambda}_{\Re}| \times |\mathbf{\Lambda}_{\Im}| = 36\,\Omega$ terms. It should be noted that to avoid division by zero in the case of $[\Lambda_{\Re 6} + \Lambda_{\Im 6}]$, the two conditions $k_1 \neq \hat{k}_1$ and $k_2 \neq \hat{k}_2$ must be satisfied.

Optimized modulation sets for IQSM for several system configurations of (L, N_t, n_R).

The proposed constellation design can be simplified as minimizing the sum term in (11), which is formulated as follows:

$$\begin{aligned} &\underset{-\sqrt{L} \le s_{k\Re}, s_{k\Im} \le \sqrt{L}}{\arg\min} \sum_{i=1}^{B} f_i \Omega_i, \\ &\qquad k = 1,...,L \\ &\text{s.t.} \sum_{k=1}^{L} |s_k|^2 = L|. \end{aligned} \tag{18}$$

Following the symmetry rule of constellation design over the in-phase and quadrature dimensions, this optimization problem can be simplified as follows:

$$\begin{aligned} &\underset{\alpha \le s_{k\Re}, s_{k\Im} \le \sqrt{L}}{\arg\min} \sum_{i=1}^{B} f_i \Omega_i, \\ &\qquad k = 1,...,L/4 \\ &\text{s.t.} \sum_{k=1}^{L/4} |s_k|^2 = L/4, \end{aligned} \tag{19}$$

where α is a positive lower bound for the real and imaginary parts that prevent them from lying on the in-phase and quadrature axes, respectively.

Based on (14) and (15), the Λ term consists of energy terms (eg, $|s_{k_{1\Re}}|^2$ and $|s_{k_{1\Im}}|^2$) and squared distance terms (eg, $|s_{k_{1\Im}} - s_{\hat{k}_{1\Im}}|^2$). For example, $\Lambda_{\Re 1}$ is the total energy of the real part and the last term $\Lambda_{\Re 6}$ is the sum of two squared ED terms. We focus on Ω_1 and Ω_{36} to explain the convergence of the proposed constellation. These terms are defined as follows:

$$\begin{aligned} \Omega_1 &= \sum_{k_1, \hat{k}_1, k_2, \hat{k}_2}^{L} \left[\Lambda_{\Re 1} + \Lambda_{\Im 1}\right]^{-n_R}, \\ \Omega_{36} &= \sum_{k_1, \hat{k}_1, k_2, \hat{k}_2}^{L} \left[\Lambda_{\Re 6} + \Lambda_{\Im 6}\right]^{-n_R}, \end{aligned} \tag{20}$$

where the weights associated with Ω_1 and Ω_{36} are f_1^2 and $f_6^2 = 1$, respectively. To minimize Ω_1, the energies of these symbols should be maximized jointly. The trivial solution to this optimization problem is to assign an equal energy with a value of one to each symbol. However, the ED between the symbols should be maximized to minimize Ω_{36}. It is known that the QAM constellation set has the maximum minimum EDs between symbols. The other terms, namely Ω_2 to Ω_{35}, are combinations of energy and squared distance terms. The weights associated with these terms depend on N_t, while $-n_R$ is present in all of the Ω terms as an exponent.

Figure 1 presents the proposed constellation sets for IQSM for several system configurations. The title of each sub-figure represents the corresponding system parameters in the following format: (L, N_t, n_R). The effects of these variables on the obtained constellations can be summarized as follows.

- As N_t increases with a fixed and relatively small value of n_R, the modulation set tends to converge to a QPSK-like shape, where $L/4$ signal symbols are gathered around the location of a conventional QPSK point in each quadrant. This is because f_1 increases more rapidly with high values of N_t, followed by f_2 and f_3. Because the Ω expressions associated with these frequencies mostly consist of symbol energy values, maximizing the minimum ED is ignored for large values of N_t.
- For a fixed and relatively small N_t, the proposed constellation converges to a QAM-like shape as n_R increases. In the QAM-like shape, the symbols are located very close to those of a conventional QAM constellation.
- The convergence of the proposed constellation to the standard shapes discussed above depends on the value of L. As L increases, the convergence in terms of N_t and n_R becomes slower.

The performance of the proposed constellation is verified in Section 8.

5 | DOUBLE QUADRATURE SPATIAL MODULATION

To improve the spectral efficiency of IQSM, we propose to transmit the real and imaginary parts of two signal symbols from a designated antenna, rather than using a combination of two antennas. Therefore, the spatial spectral efficiency of DQSM is equal to $4 \times \log_2(N_t)$, while that of IQSM is $2 \times \left\lfloor \log_2 \binom{N_t}{2} \right\rfloor$. For a large value of $N_t = 32$, DQSM and IQSM achieve spatial spectral efficiencies of 20 and 16 bpcu, respectively.

Unlike IQSM, which avoids transmitting the real/imaginary parts of signal symbols from the same antenna, DQSM does not abide by this rule. When the real/imaginary parts overlap (ie, are transmitted from the same antenna), the Euclidean space of the modulation set becomes dense, leading to performance degradation. In this case, using the same modulation set for both signal symbols leads to ambiguity at the receiver side, making it impossible to recover the signal symbols (for more details, refer to [16,17]). To overcome this problem in DQSM, we propose that the first signal symbol s_{k_1} be drawn from a constellation $\mathcal{S}_a$ and the second

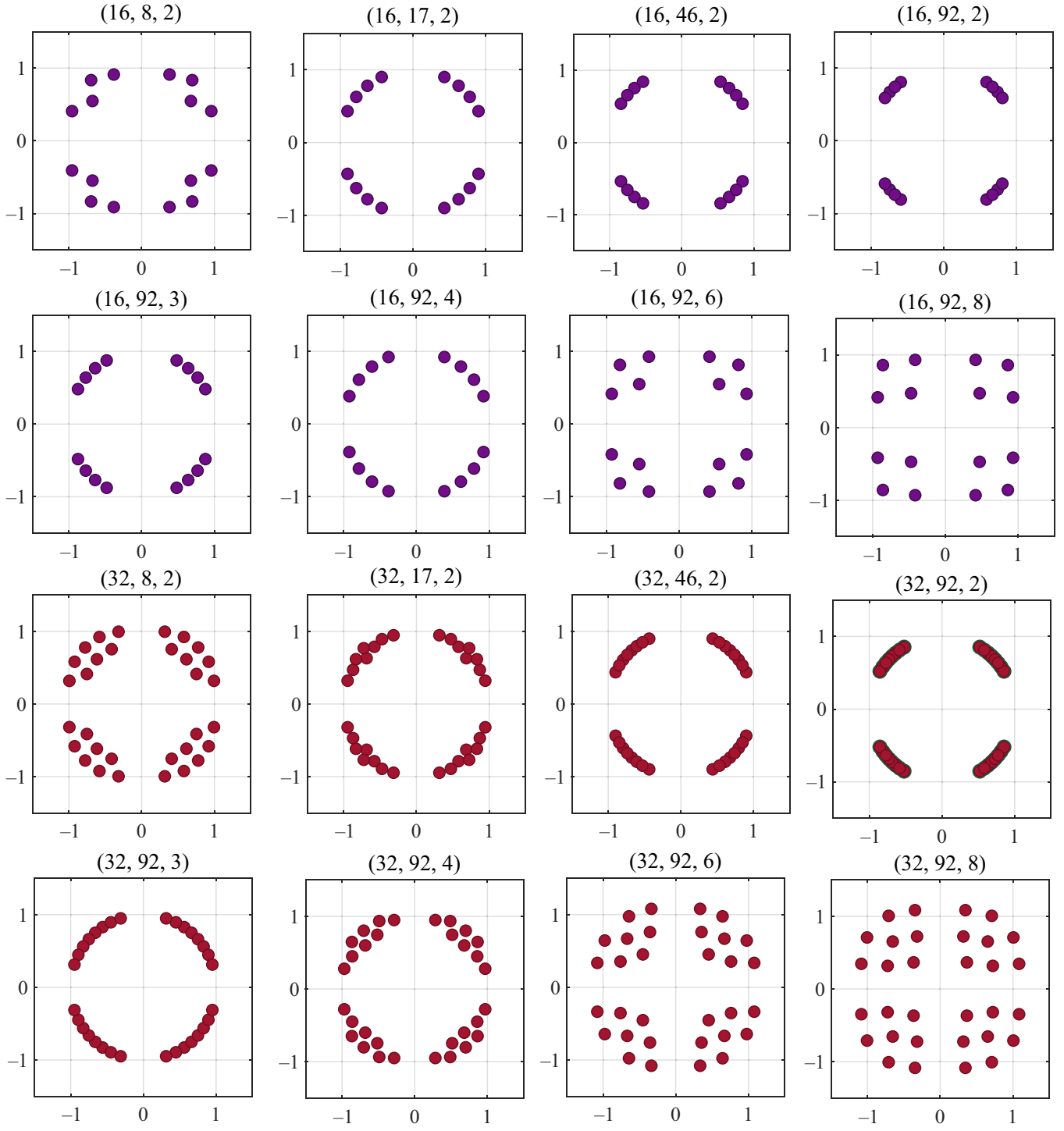

FIGURE 1 Optimized modulation sets for IQSM for several system configurations of (L, N_t, n_R)

symbol s'_{k_2} be drawn from $\mathcal{S}_b$, which can be formulated as follows:

$$\mathcal{S}_b = \left\{ s'_{k_2} = s_{k_1} e^{j\theta} | s_{k_1} \in \mathcal{S}_a \right\}, \tag{21}$$

where θ is a rotation angle. This angle is optimized by using Monte Carlo simulations to minimize the BER of the system. It is worth noting that in previous studies, signal symbols have been rotated prior to transmission to achieve higher spectral efficiency and diversity gain [32,33].

Assuming QPSK modulation, Figure 2 presents BER versus the rotation angle for several values of N_t and $n_R = 4$. The optimal rotation angle that minimizes the BER for the three simulated scenarios is approximately 25°. At each channel use, the antennas with indices $l_{1\Re}, l_{2\Re}, l_{1\Im}$, and

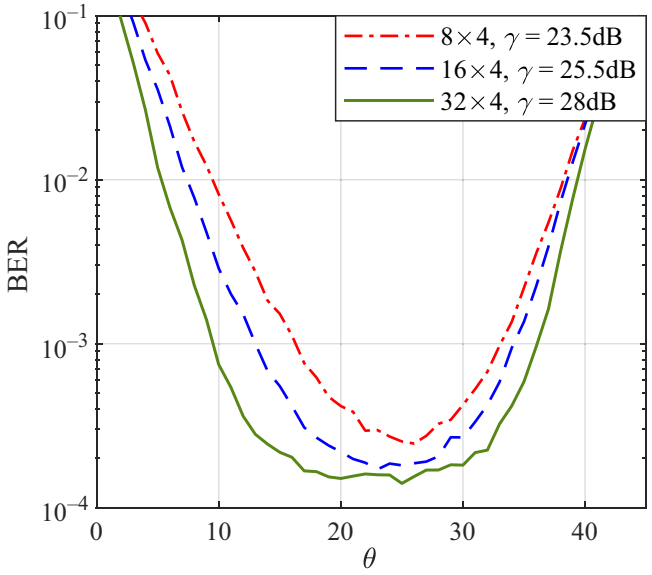

FIGURE 2 BER performance of DQSM using QPSK and $n_R = 4$ for several values of N_t

$l_{2\Im}$ are activated to transmit $s_{k_{1\Re}}, s'_{k_{2\Re}}, s_{k_{1\Im}}$, and $s'_{k_{2\Im}}$, respectively. Accordingly, DQSM achieves a spectral efficiency of $(4N_{QSM} + 2q)$. The received vector in DQSM is defined as follows:

$$\mathbf{y} = \mathbf{h}_{l_{1\Re}} s_{k_{1\Re}} + \mathbf{h}_{l_{2\Re}} s'_{k_{2\Re}} + j\mathbf{h}_{l_{1\Im}} s_{k_{1\Im}} + j\mathbf{h}_{l_{2\Im}} s'_{k_{2\Im}} + \mathbf{n}. \quad (22)$$

At the receiver, the signal and spatial symbols are recovered using the maximum likelihood (ML) detector as follows:

$$\begin{aligned} &\left(s^*_{k_{1\Re}}, s^*_{k_{1\Im}}, s'^*_{k_{2\Re}}, s'^*_{k_{2\Im}}, l^*_{1\Re}, l^*_{1\Im}, l^*_{2\Re}, l^*_{2\Im}\right) \\ &= \underset{\substack{s_{k_{1\Re}}, s_{k_{1\Im}}, s'_{k_{2\Re}}, s'_{k_{2\Im}} \\ l_{1\Re}, l_{1\Im}, l_{2\Re}, l_{2\Im}}}{\arg\min} \|\mathbf{y} - \mathbf{g}\|^2 \\ &= \underset{\substack{s_{k_{1\Re}}, s_{k_{1\Im}}, s'_{k_{2\Re}}, s'_{k_{2\Im}} \\ l_{1\Re}, l_{1\Im}, l_{2\Re}, l_{2\Im}}}{\arg\min} \|\mathbf{g}\|^2 - 2\Re\left\{\mathbf{y}^H \mathbf{g}\right\}, \end{aligned} \quad (23)$$

where $\mathbf{g} = \mathbf{h}_{l_{1\Re}} s_{k_{1\Re}} + \mathbf{h}_{l_{2\Re}} s'_{k_{2\Re}} + j\mathbf{h}_{l_{1\Im}} s_{k_{1\Im}} + j\mathbf{h}_{l_{2\Im}} s'_{k_{2\Im}}$ is the noiseless received vector in DQSM.

Table 1 lists the 15 valid conditional statements for DQSM transmission with their corresponding frequencies. Each conditional statement v_i has a probability of f_i/N_t^4. Because the real and imaginary parts are transmitted over orthogonal carriers, the performance of the system is affected only when two real or two imaginary parts are transmitted from the same antenna. Therefore, only the events $\{v_1, v_2, v_3, v_4, v_5, v_6, v_9, v_{14}\}$ can degrade DQSM performance.

TABLE 1 All possible transmission events in DQSM with their corresponding frequencies

v_i	Relational condition	f_i
v_1	$l_{1\Re} = l_{2\Re} = l_{1\Im} = l_{2\Im}$	N_t
v_2	$l_{1\Re} = l_{2\Re} = l_{1\Im} \neq l_{2\Im}$	$N_t(N_t - 1)$
v_3	$l_{1\Re} = l_{2\Re} = l_{2\Im} \neq l_{1\Im}$	$N_t(N_t - 1)$
v_4	$l_{1\Re} = l_{1\Im} = l_{2\Im} \neq l_{2\Re}$	$N_t(N_t - 1)$
v_5	$l_{2\Re} = l_{1\Im} = l_{2\Im} \neq l_{1\Re}$	$N_t(N_t - 1)$
v_6	$l_{1\Re} = l_{2\Re} \neq l_{1\Im} = l_{2\Im}$	$N_t(N_t - 1)$
v_7	$l_{1\Re} = l_{1\Im} \neq l_{2\Re} = l_{2\Im}$	$N_t(N_t - 1)$
v_8	$l_{1\Re} = l_{2\Im} \neq l_{2\Re} = l_{1\Im}$	$N_t(N_t - 1)$
v_9	$l_{1\Re} = l_{2\Re} \neq l_{1\Im} \neq l_{2\Im}$	$N_t(N_t - 1)(N_t - 2)$
v_{10}	$l_{1\Re} = l_{1\Im} \neq l_{2\Re} \neq l_{2\Im}$	$N_t(N_t - 1)(N_t - 2)$
v_{11}	$l_{1\Re} = l_{2\Im} \neq l_{2\Re} \neq l_{1\Im}$	$N_t(N_t - 1)(N_t - 2)$
v_{12}	$l_{2\Re} = l_{1\Im} \neq l_{1\Re} \neq l_{2\Im}$	$N_t(N_t - 1)(N_t - 2)$
v_{13}	$l_{2\Re} = l_{2\Im} \neq l_{1\Re} \neq l_{1\Im}$	$N_t(N_t - 1)(N_t - 2)$
v_{14}	$l_{1\Im} = l_{2\Im} \neq l_{1\Re} \neq l_{2\Re}$	$N_t(N_t - 1)(N_t - 2)$
v_{15}	$l_{1\Re} \neq l_{2\Re} \neq l_{1\Im} \neq l_{2\Im}$	$N_t(N_t - 1)(N_t - 2)(N_t - 3)$

In Table 1, the largest frequency is associated with v_{15}, where each part is transmitted from a different antenna. This means that for a large number of transmit antennas, v_{15} will be dominant, leading to significant performance improvements, meaning the performances of DQSM and IQSM will coincide. In such cases, DQSM will achieve greater spatial spectral efficiency.

Example: Let $\mathbf{x} = [0111000001111111]$, $q = 2$, and $N_t = 8$, where $\mathbf{x}$ is a message to be transmitted. According to the DQSM scheme, $\mathbf{x}$ will be divided into six parts as follows:

$$\mathbf{m}_1 = [\,0\ \ 1\,], \quad \mathbf{m}_2 = [\,1\ \ 1\,]$$
$$\mathbf{p}_{1\Re} = [\,0\ \ 0\ \ 0\,], \quad \mathbf{p}_{1\Im} = [\,0\ \ 0\ \ 1\,]$$
$$\mathbf{p}_{2\Re} = [\,1\ \ 1\ \ 1\,], \quad \mathbf{p}_{2\Im} = \begin{bmatrix} 1 & 1 & 1 \end{bmatrix}.$$

Therefore, $\mathbf{m}_1$ and $\mathbf{m}_2$ modulate $s_2 \in S_a$ and $s'_4 \in S_b$, respectively. The remaining parts modulate transmit antennas 1, 2, 8, and 8. The resulting received vector is defined as follows:

$$\mathbf{y} = \mathbf{h}_1 s_{2\Re} + j\mathbf{h}_2 s_{2\Im} + \mathbf{h}_8 \left(s'_{4\Re} + j s'_{4\Im}\right) + \mathbf{n}. \quad (24)$$

This example corresponds to v_{13} in Table 1.

6 | PARALLEL IQSM

The parallel implementation of IQSM partitions an antenna set into P equal subsets and performs IQSM independently in each subset using the same signal symbols

s_{k_1} and s_{k_2}. Each subset has $n_T = N_t/P$ transmit antennas. Consequently, the number of combinations in each subset is $\binom{n_T}{2}$. Only $2^{N_{PIQSM}}$ combinations are used for transmission in each subset, where $N_{PIQSM} = \left\lfloor \log_2 \binom{n_T}{2} \right\rfloor$. Assuming that $\mathbf{x}$ is the message to be transmitted in a given transmission instance, we split x into (2 P + 2) parts such that each $\mathbf{p}_i$ in the 2P parts is of size N_{PIQSM}. Then, $\mathbf{p}_{i_\Re}$ and $\mathbf{p}_{i_\Im}$ modulate the antenna combinations used for transmitting the real and imaginary parts in the i-th subset, where $i \in \{1, ..., P\}$. The remaining two parts $\mathbf{m}_1$ and $\mathbf{m}_2$, each of which is of size q, modulate the signal symbols s_{k_1} and s_{k_2}, respectively. The received vector is defined as follows:

$$\mathbf{y} = \frac{1}{\sqrt{P}} \sum_{i=1}^{P} \left[\mathbf{h}_{l^i_{1\Re}} s_{k_{1\Re}} + \mathbf{h}_{l^i_{2\Re}} s_{k_{2\Re}} + j\mathbf{h}_{l^i_{1\Im}} s_{k_{1\Im}} + j\mathbf{h}_{l^i_{2\Im}} s_{k_{2\Im}} \right] + \mathbf{n}, \quad (25)$$

where $\boldsymbol{l}^i_\Re = \{l^i_{1\Re}, l^i_{2\Re}\}$ and $\boldsymbol{l}^i_\Im = \{l^i_{1\Im}, l^i_{2\Im}\}$ are the antenna combinations used to transmit the real and imaginary parts in the i-th subset. Because IQSM uses antenna combinations to alleviate the power-of-two constraint on N_t, the size of n_T can also be any arbitrary number. Therefore, the spectral efficiency of PIQSM is defined as $2\left(P \times N_{PIQSM} + q\right)$.

The ML detector is employed on the receiver side to recover the spatial and signal symbols as follows:

$$\begin{aligned} &\left(s^*_{k_{1\Re}}, s^*_{k_{2\Re}}, s^*_{k_{1\Im}}, s^*_{k_{2\Im}}, \left\{l^{1*}_\Re, l^{1*}_\Im, ..., l^{P*}_\Re, l^{P*}_\Im\right\}\right) \\ &= \underset{\substack{s_{k_{1\Re}}, s_{k_{2\Re}}, s_{k_{1\Im}}, s_{k_{2\Im}} \\ l^1_\Re, l^1_\Im, ..., l^P_\Re, l^P_\Im}}{\arg\min} \|\mathbf{y} - \mathbf{g}\|^2 \\ &= \underset{\substack{s_{k_{1\Re}}, s_{k_{2\Re}}, s_{k_{1\Im}}, s_{k_{2\Im}} \\ l^1_\Re, l^1_\Im, ..., l^P_\Re, l^P_\Im}}{\arg\min} \|\mathbf{g}\|^2 - 2\Re\left\{\mathbf{y}^H \mathbf{g}\right\}, \end{aligned} \quad (26)$$

where $\mathbf{g} = \left(1/\sqrt{P}\right) \sum_{i=1}^{P} \left[\mathbf{h}_{l^i_{1\Re}} s_{k_{1\Re}} + \mathbf{h}_{l^i_{2\Re}} s_{k_{2\Re}} + j\mathbf{h}_{l^i_{1\Im}} s_{k_{1\Im}} + j\mathbf{h}_{l^i_{2\Im}} s_{k_{2\Im}} \right]$ is the noiseless received vector in PIQSM. Because the spatial spectral efficiency increases linearly with P, PIQSM reduces the N_t value required to achieve a given spectral efficiency while requiring the same number of RF chains as IQSM (two RF chains).

Example: Let $\mathbf{x} = [0011000101001110]$, $q = 2$, $P = 2$, and $N_t = 10$. Then, x is split into six parts, which are defined as follows:

$$\mathbf{m}_1 = [\ 0\ \ 0\ ], \quad \mathbf{m}_2 = [\ 1\ \ 1\ ]$$
$$\mathbf{p}_{1\Re} = [\ 0\ \ 0\ \ 0\ ], \quad \mathbf{p}_{1\Im} = [\ 1\ \ 0\ \ 1\ ]$$
$$\mathbf{p}_{2\Re} = [\ 0\ \ 0\ \ 1\ ], \quad \mathbf{p}_{2\Im} = [\ 1\ \ 1\ \ 0\ ].$$

Table 2 contains the PIQSM antenna mapping for $N_t = 10$ and $P = 2$. In this example, $\mathbf{m}_1$ and $\mathbf{m}_2$ modulate s_1 and s_4, respectively. In the first group, $\mathbf{p}_{1\Re}$ and $\mathbf{p}_{1\Im}$ are used to choose $\boldsymbol{l}^1_\Re = \{1, 2\}$ and $\boldsymbol{l}^1_\Im = \{2, 4\}$. Similarly, $\mathbf{p}_{2\Re}$ and $\mathbf{p}_{2\Im}$ are used to choose $\boldsymbol{l}^2_\Re = \{6, 8\}$ and $\boldsymbol{l}^2_\Im = \{7, 10\}$ from the second subset. Accordingly, the received vector is defined as follows:

$$\begin{aligned} \mathbf{y} = \frac{1}{\sqrt{2}} &\left[s_{1\Re} \left(\mathbf{h}_1 + \mathbf{h}_6\right) + s_{4\Re} \left(\mathbf{h}_2 + \mathbf{h}_8\right) \right. \\ &\left. + j s_{1\Im} \left(\mathbf{h}_2 + \mathbf{h}_7\right) + j s_{4\Im} \left(\mathbf{h}_4 + \mathbf{h}_{10}\right) \right] + \mathbf{n}. \end{aligned} \quad (27)$$

Table 3 provides a comparison between several spatial modulation systems in terms of the number of transmit antennas required to achieve a given spatial spectral efficiency M_{spa}. It is clear that PIQSM requires the smallest number of transmit antennas, followed by DQSM and IQSM.

TABLE 2 Example of PIQSM mapping for $P = 2$ and $N_t = 10$

Information bits	l^1	l^2
000	{1, 2}	{6, 7}
001	{1, 3}	{6, 8}
010	{1, 4}	{6, 9}
011	{1, 5}	{6, 10}
100	{2, 3}	{7, 8}
101	{2, 4}	{7, 9}
110	{2, 5}	{7, 10}
111	{3, 4}	{8, 9}

TABLE 3 Numbers of transmitting antennas required to achieve the same spatial spectral efficiency (M_{spa}) for several systems

M_{spa}	MA-SM	QSM	IQSM	DQSM	PIQSM ($P = 2$)
12	92	64	12	8	10
16	363	265	24	16	14
20	1449	1024	46	32	18

7 | COMPLEXITY ANALYSIS

In this section, we discuss the receiver complexity for the proposed DQSM and PIQSM schemes in comparison to IQSM. It is clear from (3) and (22) that the complexity of IQSM and DQSM

TABLE 4 Receiver Computational Complexity for IQSM and DQSM

Term	Real multiplications	Real additions
$\mathbf{g}$	$8n_R$	$6n_R$
$\|\mathbf{y} - \mathbf{g}\|^2$	$2n_R$	$4n_R - 1$
Total	$10n_R$	$10n_R - 1$

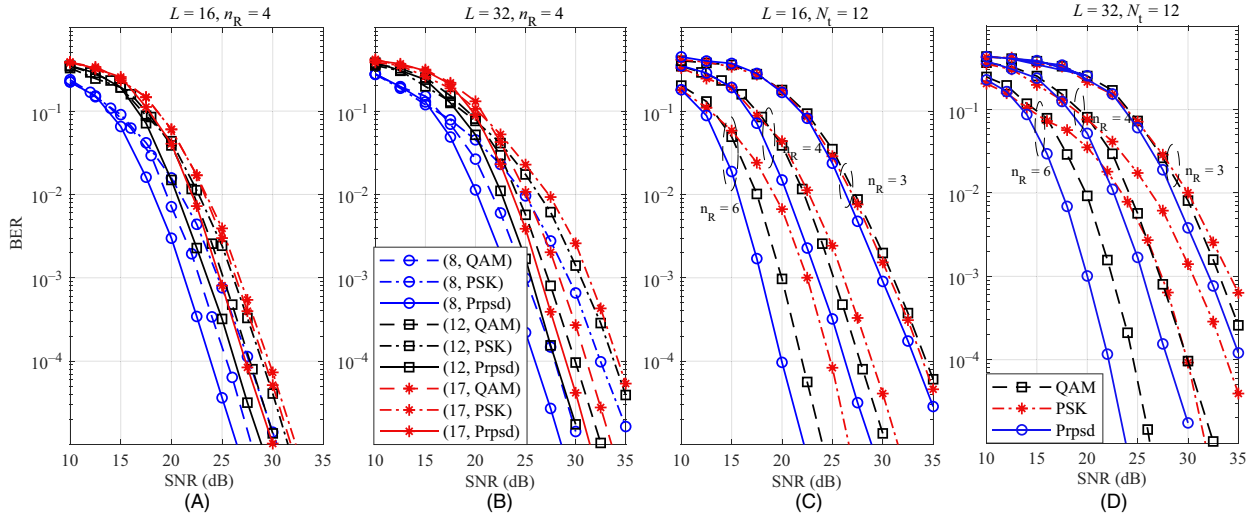

FIGURE 3 BER performance of IQSM using the proposed modulation set, QAM, and PSK for several values of N_t with (A) $L = 16$ and (B) $L = 32$, and several values of nR with (C) $L = 16$ and (D) $L = 32$. The values in the legend entries for (B) represent N_t

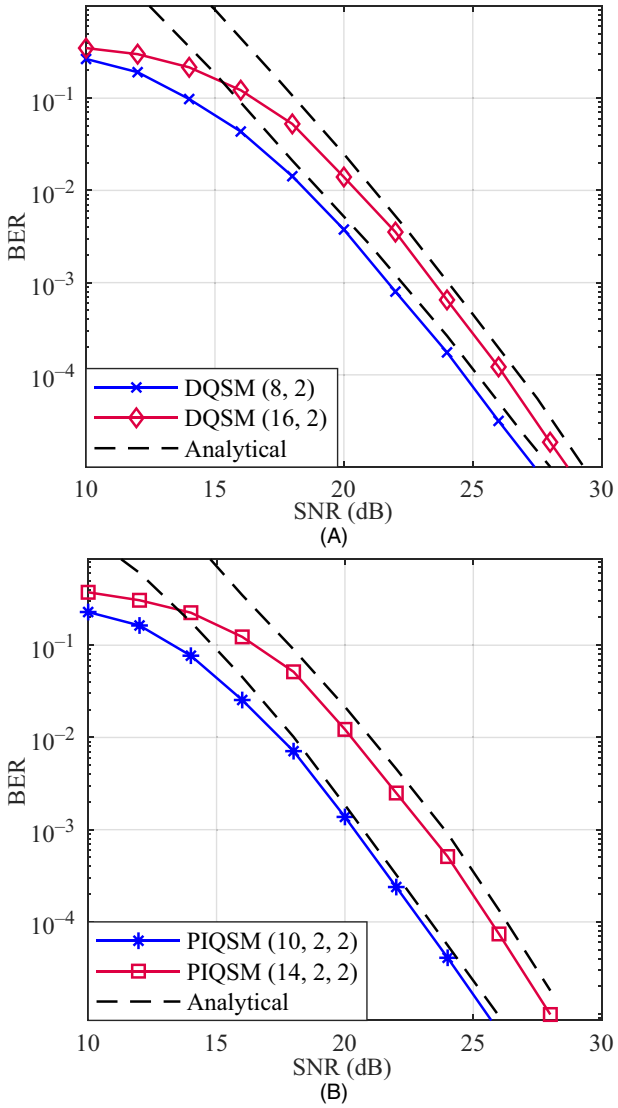

FIGURE 4 Validation of simulation results for (A) DQSM and (B) PIQSM versus analytical results

is identical for the same spectral efficiency. Because the rotation angle in Figure 2 is obtained offline, the optimization process does not incur any computational cost for the DQSM receiver. Table 4 lists the computational complexities of IQSM and DQSM.

For a target spectral efficiency of M, the ML search is performed over an M-dimensional space. Therefore, IQSM and DQSM require the following numbers of real multiplications and additions:

$$\eta_{\text{mul}} = \left(10n_{\text{R}}\right) 2^{M} \quad \eta_{\text{add}} = \left(10n_{\text{R}} - 1\right) 2^{M}. \tag{28}$$

Because the same two signal symbols are transmitted from P antenna subsets in PIQSM, the number of multiplications performed by a PIQSM receiver is identical to those in IQSM and DQSM, and the number of additions is only increased by $4n_{\text{R}}\,(2P-2)$. One advantage of PIQSM compared to IQSM is the reduced number of transmit antennas. This reduces the channel estimation overhead in terms of system resources, time, and frequency.

It is well known that the ML detector achieves optimal performance at the cost of high computational complexity. Several studies have investigated low-complexity detectors for QSM-based systems [26,34,35]. In the future, we would like to propose low-complexity detection algorithms that consider the specific structures of the proposed DQSM and PIQSM schemes.

8 | SIMULATION RESULTS

In this section, the channel state information is assumed to be perfectly known only by the receiver. In all simulated scenarios, $n_{\text{R}} = 4$, unless stated otherwise.

Figure 3 presents a performance comparison between IQSM with the proposed constellation versus IQSM with the conventional schemes (QAM/PSK). Both Figure 3A,B have the same legend entries, where the numbers in the entries represent N_t. Additionally, Figures 3C and 3D have the same legend entries. Based on the results presented in Figure 3, we can draw the following conclusions.

1. For a fixed $L=16$ and $n_R=4$ (Figure 3A): The proposed constellation outperforms both QAM and PSK for all simulated values of N_t. Compared to QAM, the proposed constellation has a gain of 1.5 dB for $N_t=8$ and 12, and a gain of 2 dB for $N_t=17$. The proposed constellation outperforms PSK by approximately 3 dB for $N_t=8$ and 12, and by 2.5 dB for $N_t=17$. Based on this performance trend, we can conclude that the proposed constellation converges to the PSK modulation set for large values of N_t.
2. For a fixed $L=32$ and $n_R=4$ (Figure 3B): The proposed constellation outperforms the QAM constellation by approximately 2 dB for $N_t=8,12$, and 17. Compared to PSK, the proposed constellation has gains of 6 dB for $N_t=8$ and 12, and a gain of 5 dB for $N_t=17$. As L increases, the convergence of the optimal constellation to a PSK-like shape occurs at relatively large values of N_t.
3. For a fixed $L=16$ and $N_t=12$ (Figure 3C): At small values of n_R, such as $n_R=3$, the performance gap between the three constellations is small. In this case, the QAM constellation exhibits the worst performance. As n_R increases, for $n_R=4$ and 6, the proposed constellation outperforms PSK and QAM by approximately 2.7 dB and 1.5 dB, respectively, for $n_R=4$, and by 2 dB and 5 dB, respectively, for $n_R=6$. The performance of QAM is improved because the squared distance term becomes dominant as n_R increases. This is also why the PSK constellation, which requires maximizing symbol energy, has the worst performance.
4. For a fixed $L=32$ and $N_t=12$ (Figure 3D): Similar to the results in Figure 3C, the proposed constellation outperforms QAM by approximately 1 dB, 2 dB, and 2.5 dB for $n_R=3,4$, and 6, respectively. The PSK constellation lags behind the performance of the proposed constellation by 2 dB, 6 dB, and 8 dB for $n_R=3,4$, and 6, respectively. The performance gap between the PSK constellation and proposed constellation increases as n_R increases.

In Figure 4, the analytical results for the upper bound of the bit-error rate performance of the proposed schemes, namely DQSM and PIQSM, are compared to the simulation results. The derived formulae coincide with the simulations, especially at high SNR values (asymptotic performance). We now analyze the performance of the proposed DQSM and PIQSM schemes with IQSM and MA-SM, where all systems require two RF chains. The performance of these systems was evaluated at the same total spectral efficiency.

Figure 5A presents the performance of IQSM and DQSM using QPSK modulation for several different numbers of transmit antennas. Based on Figure 2, the rotation angle in the DQSM system is set to 25°. In this scenario, DQSM requires 4, 8, and 14 fewer transmit antennas compared to IQSM to achieve spectral efficiencies of 16, 20, and 24 bpcu, respectively. We can also conclude that for small values of N_t, the performance gap between IQSM and DQSM is large. This is because the probability of transmitting the real/imaginary parts from the same antenna is high for small N_t

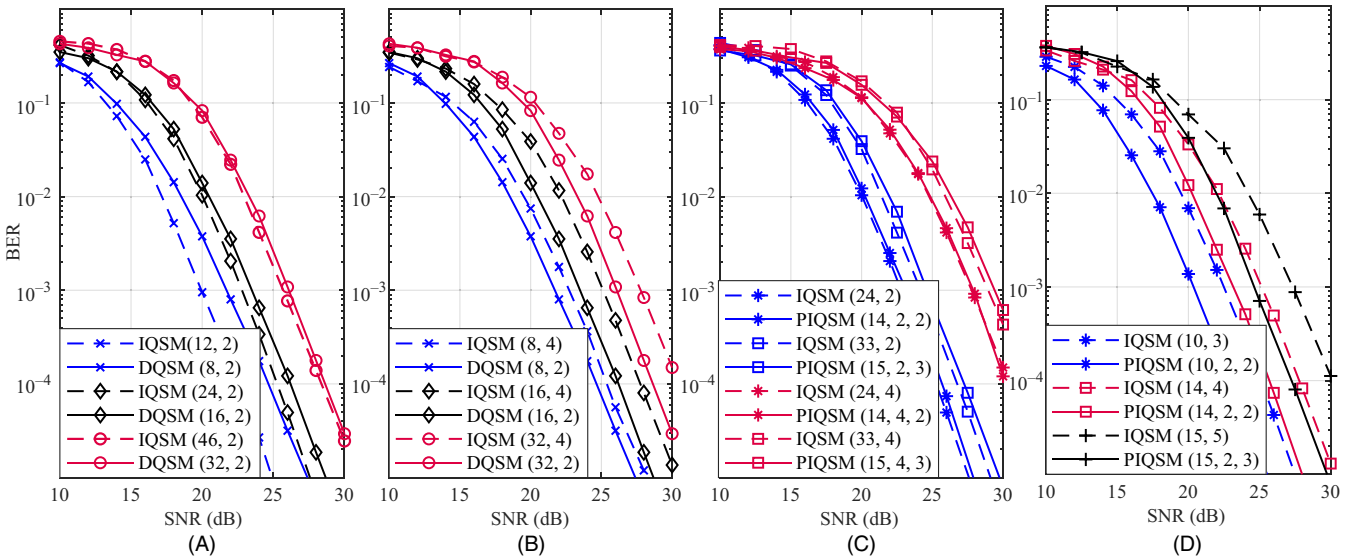

FIGURE 5 BER performances of IQSM compared to (A) DQSM for the same q, (B) DQSM for the same N_t, (C) PIQSM for the same q, and (D) PIQSM for the same N_t using $P=2$ and 3. The legend entries indicate that (N_t, q) for all schemes and (N_t, q, P) for PIQSM

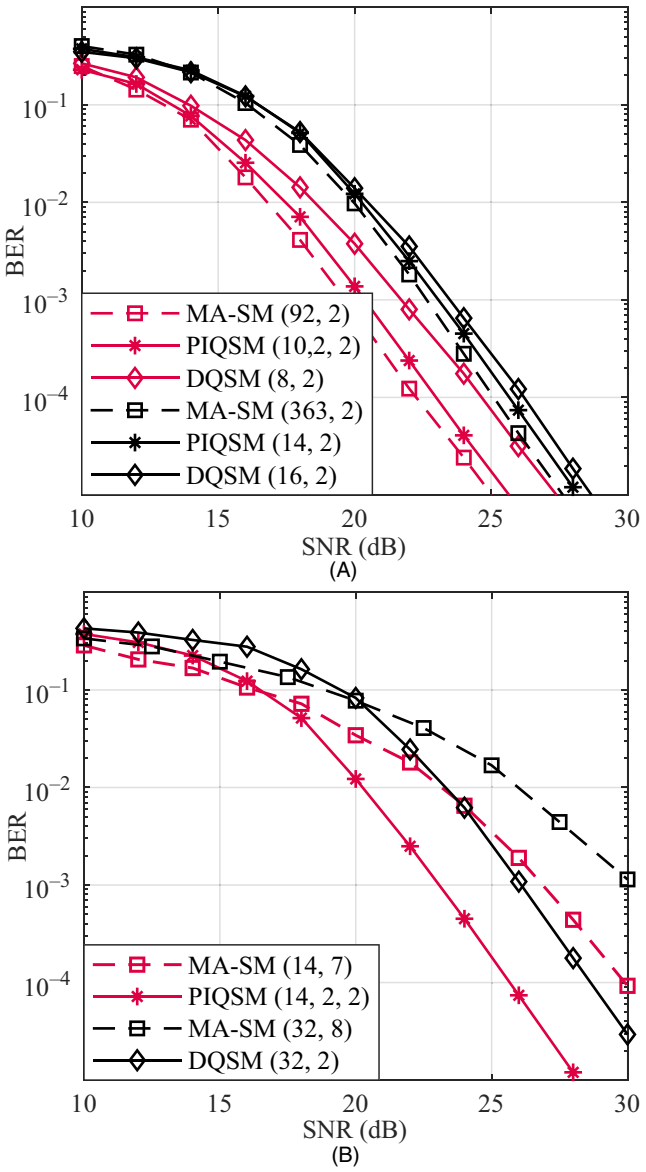

FIGURE 6 BER performance comparison between (A) DQSM, PIQSM, and MA-SM for the same q, (B) PIQSM and MA-SM, and DQSM and MA-SM for the same N_t. The legend entries represent (N_t, q) for all schemes and (N_t, q, P) for PIQSM

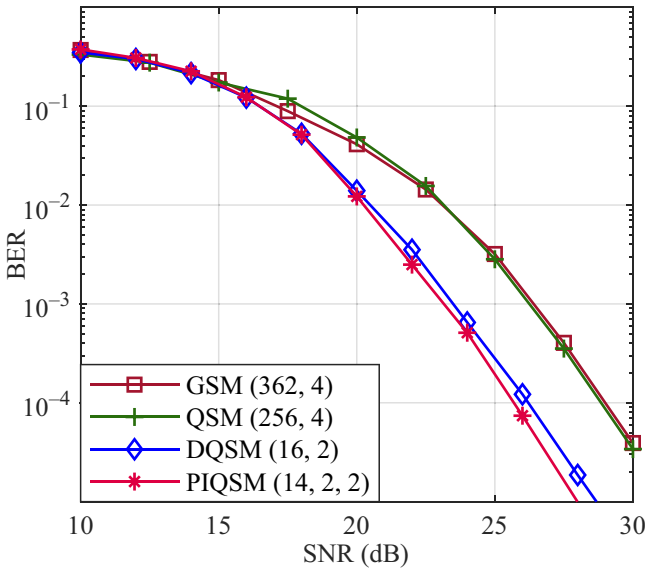

FIGURE 7 BER comparison between DQSM, PIQSM, GSM, and QSM. The legend entries represent (N_t, q) for all schemes and (N_t, q, P) for PIQSM

values, as discussed in Section 5. However, as N_t increases, the overlapping probability decreases, leading to a significant performance improvement for DQSM. The case in which DQSM uses $N_t = 32$ and IQSM uses $N_t = 46$ is where the performances of both algorithms coincide at high SNRs. For the same number of transmit antennas, DQSM outperforms IQSM in all of the scenarios depicted in Figure 5B. For example, DQSM outperforms IQSM by 2 dB at a target BER of 2×10^{-4} with $N_t = 32$.

Based on the results presented in Figure 5C for $P = 2$, PIQSM achieves a result of $M_{spa} = 16$ bpcu with $N_t = 14$ with 10 fewer antennas than IQSM. Similarly, PIQSM with $P = 3$ reduces the number of transmit antennas required to achieve $M_{spa} = 18$ by 18. For all the simulated scenarios in this figure, the two schemes exhibit very similar performance. For example, the curves perfectly coincide when $N_t = 14$, $P = 2$, and $q = 4$ for PIQSM. For the same N_t, PIQSM outperforms IQSM for all of the simulated scenarios presented in Figure 3D. This improvement reaches up to 2 dB and 3 dB for $P = 2$ and $P = 3$, respectively.

In Figure 6A, we compare the performances of DQSM, PIQSM, and MA-SM. Assuming the use of QPSK, MA-SM, DQSM, and PIQSM deploy 92, 8, and 10 antennas, respectively, to achieve a spectral efficiency of $M = 16$ bpcu. Additionally, MA-SM, DQSM, and PIQSM require 363, 16, and 14 antennas, respectively, to achieve a spectral efficiency of $M = 20$ bpcu. As shown in Figure 6A, MA-SM outperforms DQSM and PIQSM by 2 dB and 0.7 dB, respectively, when $M = 16$ bpcu. As the number of antennas increases, the performance gaps decrease to approximately 1 dB for DQSM and 0.5 dB for PIQSM when $M = 20$ bpcu. This implies that the proposed schemes are more effective for large-scale MIMO systems because they require a fraction of the N_t values required by MA-SM. In Figure 6B, we compare the performances of MA-SM and PIQSM for targets of $M = 20$ bpcu and $N_t = 14$. Additionally, a comparison to DQSM is presented for $M = 24$ bpcu and $N_t = 32$. In both cases, the proposed algorithms outperform MA-SM by approximately 4 dB.

Finally, we compare the performances of the proposed DQSM and PIQSM to those of GSM and QSM for a target of $M = 20$ bpcu in Figure 5. While GSM and QSM provide similar performance, DQSM and PIQSM outperform these methods by approximately 2.5 dB and 3 dB, respectively. Furthermore, DQSM requires 347 and 240

fewer transmit antennas than GSM and QSM, respectively. Similarly, PIQSM reduces the required numbers of transmit antennas by 349 and 242 compared to GSM and QSM, respectively.

9 | CONCLUSIONS

The main contributions of this paper can be summarized as follows. First, we derived an upper bound for the pairwise error probability of an IQSM system. The design of a constellation was then modeled as a multivariate optimization problem to minimize the asymptotic error probability. The proposed constellation outperformed QAM and PSK on all simulated scenarios. We then introduced the DQSM scheme, where each of the real and imaginary parts of two signal symbols are transmitted from a designated antenna. In our design, the two signal symbols in DQSM are drawn from two different modulation sets. The second modulation set is a rotated version of the first set, where the rotation angle is optimized to minimize the BER based on Monte Carlo simulations. Finally, we proposed a PIQSM scheme that splits a transmit antenna set into equal subsets. Conventional IQSM is then performed independently in each subset using the same two signal symbols. Compared to IQSM, DQSM requires a smaller number of transmit antennas to achieve a given spectral efficiency and their error performances coincide at large numbers of transmit antennas. PIQSM and IQSM perform similarly, but the former requires a fraction of the transmit antennas required by the latter. Furthermore, DQSM and PIQSM outperform IQSM by up to 2 dB and 3 dB, respectively, for the same number of transmit antennas.

ORCID


Manar Mohaisen https://orcid.org/0000-0002-7270-0933

REFERENCES

1. E. Basar et al., *Index modulation techniques for next-generation wireless networks*, IEEE Access **5** (2017), 16693–16746.
2. X. Cheng et al., *Index modulation for 5G: striving to do more with less*, IEEE Wireless Commun. **25** (2018), 126–132.
3. R. Mesleh et al., *Spatial modulation*, IEEE Trans. Veh. Technol. **57** (2008), no. 4, 2228–2241.
4. J. Jeganathan, A. Ghrayeb, and L. Szczecinski, *Spatial modulation: optimal detection and performance analysis*, IEEE Commun. Lett. **12** (2008), no. 8, 545–547.
5. M. Maleki et al., *On the performance of spatial modulation: optimal constellation breakdown*, IEEE Trans. Commun. **62** (2013), no. 1, 144–157.
6. M. Maleki, H. R. Bahrami, and A. Alizadeh, *Constellation design for spatial modulation*, in Proc. IEEE Int. Conf. Commun. (London, UK), 2015, pp. 2739–2743.
7. R. Mesleh, O. Hiari, and A. Younis, *Generalized space modulation techniques: hardware design and considerations*, Phys. Commun. **26** (2018), 87–95.
8. M. Wen et al., *A survey on spatial modulation in emerging wireless systems: Research progresses and applications*, IEEE J. Sel. Areas Commun. **37** (2019), no. 9, 1949–1972.
9. A. Younis et al., *Generalised spatial modulation*, in Proc. Conf. Record Asilomar Conf. Signals, Syst. Comput. (Pacific Grove, CA, USA), 2010, pp. 1498–1502.
10. J. Wang, S. Jia, and J. Song, *Generalised spatial modulation mystem with multiple active transmit antennas and low complexity detection scheme*, IEEE Trans. Wireless Commun. **11** (2012), no. 4, 1605–1615.
11. R. Mesleh, S. S. Ikki, and H. M. Aggoune, *Quadrature spatial modulation*, IEEE Trans. Veh. Technol. **64** (2014), no. 6, 2738–2742.
12. I. Al-Nahhal, O. A. Dobre, and S. S. Ikki, *Quadrature spatial modulation decoding complexity: Study and reduction*, IEEE Wireless Commun. Lett. **6** (2017), no. 3, 378–381.
13. B. T. Vo, H. H. Nguyen, and H. D. Tuan, *Constellation design for quadrature spatial modulation*, in Proc. IEEE Veh. Technol. Conf. (Toronto, Canada), 2017, pp. 1–5.
14. J. Li et al., *Generalized precoding-aided quadrature spatial modulation*, IEEE Trans. Veh. Technol. **66** (2016), no. 2, 1881–1886.
15. F. R. Castillo-Soria et al., *Extended quadrature spatial modulation for MIMO wireless communications*, Phys. Commun. **32** (2019), 88–95.
16. M. Mohaisen and S. Lee, *Complex quadrature spatial modulation*, ETRI J. **39** (2017), 514–524.
17. M. Mohaisen, *Increasing the minimum Euclidean distance of the complex quadrature spatial modulation*, IET Commun. **12** (2018), no. 7, 854–860.
18. A. Iqbal, M. Mohaisen, and K. S. Kwak, *Modulation set optimization for the improved complex quadrature SM*, Wireless Commun. Mobile Comput. **2018** (2018), 1–12.
19. M. Mohaisen, *Generalized complex quadrature spatial modulation*, Wireless Commun. Mobile Comput. **2019** (2019), 3137927:1–12.
20. B. Vo and H. H. Nguyen. *Improved quadrature spatial modulation*, in Proc. IEEE Veh. Technol. Conf. (Toronto, Canada), 2017, pp. 1–5.
21. P. Ju et al., *Generalized spatial modulation with transmit antenna grouping for correlated channels*, in Proc. IEEE Int. Conf. Commun. (Kuala Lumpur, Malaysia), May 2016, pp. 1–6.
22. S. AbuTayeh et al., *A half-full transmit-diversity spatial modulation scheme*, in Proc. Int. Conf. Broadband Commun., Netw. Syst. (Faro, Portugal), 2018, pp. 257–266.
23. W. Qu et al., *Generalized spatial modulation with transmit antenna grouping for Massive MIMO*, IEEE Access **5** (2017), 26798–26807.
24. L. Xiao et al., *Compressed-sensing assisted spatial multiplexing aided spatial modulation*, IEEE Trans. Wireless Commun. **17** (2017), no. 2, 794–807.
25. M. Mohaisen, *Constellation design and performance analysis of the parallel spatial modulation*, Int. J. Commun. Syst. **32** (2019), no. 18, e4165.
26. F. R. Castillo-Soria et al., *Generalized quadrature spatial modulation scheme using antenna grouping*, ETRI J. **39** (2017), no. 5, 707–717.
27. G. Huang et al., *Parallel quadrature spatial modulation for massive MIMO systems with ICI avoidance*, IEEE Access **7** (2019), 154750–154760.
28. S. Oladoyinbo, N. Pillay, and H. Xu, *Single-Symbol generalized quadrature spatial modulation*, Wireless Commun. Mobile Comput. **2019** (2019), 3137927:1–12.

29. T. Holoubi et al., *Double quadrature spatial modulation*, Int. J. Internet, Broadcast. Commun. **11** (2019), no. 3, 27–33.
30. M. K. Simon and M. S. Alouini, Digital communication over fading channels, 2nd ed., vol. **95**, John Wiley & Sons, Hoboken, New Jersey, 2005.
31. G. Gritsch, H. Weinrichter, and M. Rupp, *A union bound of the bit error ratio for data transmission over correlated wireless mimo channels*, in Proc. IEEE Int. Conf. Acoustics, Speech, Signal Process. (Montreal, Canada), May 2004, pp. 405–408.
32. J. Li et al., *Layered orthogonal frequency division multiplexing with index modulation*, IEEE Syst. J. **13** (2019), no. 4, 3793–3802.
33. N. Muchena et al., *Rotated-symbol generalized spatial modulation*, Int. J. Internet, Broadcast. Commun. **11** (2019), no. 3, 34–40.
34. L. Gou, J. Ge, and Y. Cao, *Low-complexity sphere decoding for quadrature spatial modulation*, in Proc. IEEE Veh. Technol. Conf. (Porto, Portugal), June 2018, pp. 1–5.
35. I. Al-Nahhal, O. A. Dobre, and S. Ikki, *Low complexity decoders for spatial and quadrature spatial modulations-invited paper*, in Proc. IEEE Veh. Technol. Conf. (Porto, Portugal), June 2018, pp. 1–5.

AUTHOR BIOGRAPHIES

Tasnim Holoubi received her bachelor's degree in information systems from Al-Jouf University, Saudi Arabia in 2018. She is currently pursuing a master's degree in communication engineering at the Korea University of Technology and Education, Korea. Her research interests include MIMO systems, spatial modulation, and signal constellation design.

Sheriff Murtala received his bachelor's degree in electrical engineering from the University of Ilorin, Nigeria in 2010. He completed his master's degree in communication engineering at the Federal University of Technology, Minna, Nigeria in 2017. He is currently pursuing a PhD in information and communication engineering at the Korea University of Technology and Education, Korea. His research interests include MIMO systems, spatial modulation, social network analysis, computer vision, and artificial intelligence.

Nishal Muchena received his bachelor of technology degree from the Harare Institute of Technology, Zimbabwe in 2014. He is currently pursuing a master's degree in electronics and communication engineering at the Korea University of Technology and Education, Korea. His research interests include MIMO systems with a special focus on spatial modulation, constellation design, and high-efficiency modulation techniques.

Manar Mohaisen received his masterâ€™s degree in communications and signal processing from the University of Nice-Sophia Antiplois, France in 2005 and his PhD in communications engineering from Inha University, Seoul, Korea in 2010. From 2001 to 2004, he worked as a cell planning engineer at the Palestinian Telecommunications Company. From 2010 to 2019, he was a full-time lecturer and assistant professor in the department of EEC Engineering, Korea Tech, Korea. Since August 2019, he has worked as an assistant professor in the Department of Computer Science at Northeastern Illinois University. His research interests include wireless communications with a focus on MIMO systems and social network analysis.